Water Practice & Technology

IWA PUBLISHING

Water Practice & Technology Vol 17 No 8, 1742 doi: 10.2166/wpt.2022.080

Development and characterization of N-substituted derivative of 2-sulfanylacetamide on *Phyllanthus emblica* seed coat as novel adsorbent for remediation of As(III) from water

Madhvi Nayyar, Rajeev Kumar* and Jyoti Chawla
Manav Rachna International Institute of Research and Studies, Faridabad, Haryana, India
*Corresponding author. E-mail: rajeevkumar.fet@mriu.edu.in

RK, 0000-0002-0820-5970

ABSTRACT

Primary aliphatic or aromatic amino acids on *Phyllanthus emblica* seed coat are derivatized in the form of N-substituted 2-sulfanylacetamide derivative. Pristine *P. emblica* (PPE) and derivatized *P. emblica* (DPE) products were used for removal of trivalent arsenic from aqueous sample. Thioglycolic acid and 1-ethyl-3-(3-dimethylaminopropyl) carbodiimidehydrochloride (EDC) were used for the derivatization process. The carboxylic group of thioglycolic acid reacts with EDC to form an activated ester leaving group, which is displaced by nucleophilic attack of primary amino acids on seed coat. The BET surface area (0.3152 ± 0.0081 m^2/g) and Langmuir surface area (0.3571 ± 0.0054 m^2/g) of PPE are changed after modification. DPE showed high surface area compared to un-derivatized adsorbent due to presence of more modified groups on the surface (BET surface area 0.5812 m^2/g, Langmuir surface area 0.6372 m^2/g). Infrared and EDX studies confirmed modification of prepared material. The batch study was carried out by using 0.06 g/L of adsorbent dose at pH 7 for 120 minutes of contact time. The Langmuir q_{max} for PPE and DPE were observed to be 76.92 and 90.90 mg/g respectively.

Key words: 2-sulfanylacetamide, adsorption, arsenic removal, isotherms, *Phyllanthus emblica*

HIGHLIGHTS

- Facile modification on *P. emblica* seed coat.
- N-substituted derivative of 2-sulfanylacetamide.
- Trivalent arsenic has high affinity for sulfhydryl groups.
- Removal of trivalent arsenic from aqueous sample.
- Characterized by IR, SEM, EDX, and XRD techniques.

GRAPHICAL ABSTRACT

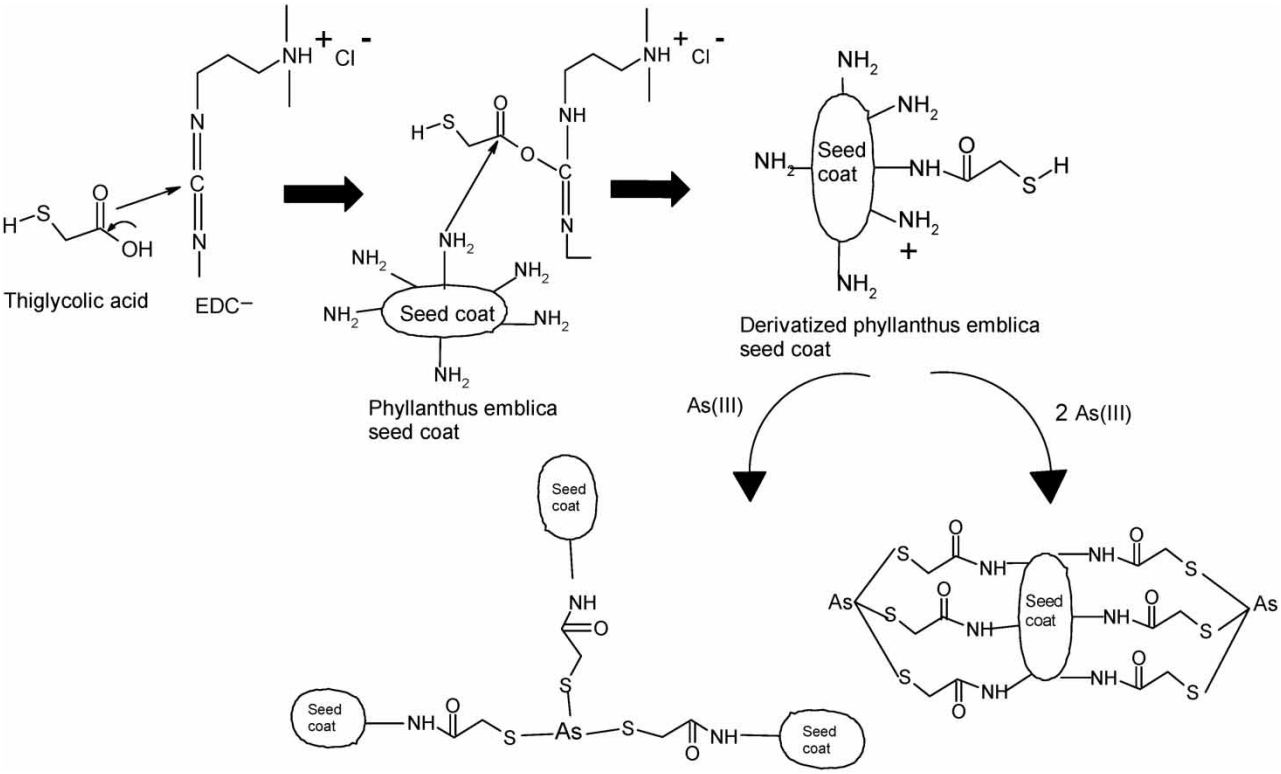

1. INTRODUCTION

Increasing use of various forms of arsenic in different fields is intimidation to the environment as well as human health. Trivalent arsenic is mainly used in pesticides, insecticides, herbicides, and treated wood products. Arsenic contamination in drinking water is a global problem, affecting millions of people. The US Environmental Protection Agency and World Health Organization consider that all forms of arsenic cause human health implications. Arsenic is number one for hazardous ions as per US-ATSDR (Agency for Toxic Substances and Disease Registry) and group 'A' carcinogen material in its priority list issued in 2001. Many studies have confirmed the toxicity of arsenite (Mandal & Suzuki 2002; Osuna-Martínez *et al.* 2021). According to EPA and WHO guidelines the concentration of arsenic in public water supply should be less than 0.01 mg/L (USEPA 2001; WHO 2011). India, Bangladesh, Canada, Chile, China, Cambodia, Germany, Japan, USA, Thailand, and Mexico are severely affected with arsenic contamination (Bagchi 2007).

Arsenic contamination has affected number of places throughout the world. India as well as other international countries such as Bangladesh, Canada, Chile, China, Cambodia, Germany, Japan, USA, Thailand, and Mexico are rigorously affected with arsenic contamination (Bagchi 2007; Shaji *et al.* 2020). More than 238 million people in 21 states in India were affected by a high level of arsenic in usable water as per Times of India report (Jadhav 2017). More than 70 million people in 96 districts in 12 States in India were affected by high level of arsenic in water as per India Today report (ITWD 2018). As per a recent article in Science News published on May 21st, 2020 regarding the risk of arsenic contaminated water, more than 220 million people may be at high risk around the world (Gramling 2020). Arsenic concentration above the recommended limit can causes severe health effects such as abdominal pain, diabetes, pulmonary disease, diarrhea, cardiovascular disease, and cancer (Palma-Lara *et al.* 2020).

Many methods have been proposed for the removal of dissolved arsenic ions from water (Nicomel *et al.* 2016; Alka *et al.* 2021). An adsorption technique is widely used because of effective cost but it becomes necessary to explore cost effective and efficient materials for adsorption or removal of metals especially heavy metals and apart from good adsorption, efficient regeneration of adsorbent should be feasible up to certain cycles (Saini *et al.* 2018, 2019).

A wide range of bulk and nano-materials have been synthesized and modified for removal of arsenic trivalent ions from water (Balsamo *et al.* 2010; Natale *et al.* 2013; Hu *et al.* 2017). Different iron oxide coated sand (0.041–0.136 mg/g adsorption capacity) (Thirunavukkarasu *et al.* 2005), MnO_2 loaded resin (53) (Lenoble *et al.* 2004), Oxisol (2.6) (Ladeira & Ciminelli 2004), activated alumina grains (3.48) (Lin & Wu 2001), nanoscale zero-valent iron (2.47) (Kanel *et al.* 2005), hydrous titanium dioxide (33.4), nanocrystalline TiO_2 (37.5) (Pirilä *et al.* (2011), α-Fe_2O_3 (1.9) (Prasad *et al.* (2011)), CuO (26.9) (Martinson & Reddy (2009), polymer nanocomposite (Fe_3O_4) (2.83) (Vunain *et al.* (2013)) and many other metallic oxide as well as activated carbon have been widely applied as adsorbent for removal of trivalent arsenic from water (Mohan & Pittman 2007). The main disadvantages of these synthesized adsorbents are high cost, low removal efficiency, and more hazardous towards the environment. To overcome these problems natural and modified natural materials have been proposed and applied for removal of arsenic from water. Rice husk biochar (19.3), *Hydrilla verticilata* (11.65), tea waste (7.36), pomegranate peel (5.57), corn cob (4.33), bagasse (1.35), mango bark (1.25), orange peel (OP) (1.08), biochar of rice straw (0.44), and banana peel (0.84) are used as natural adsorbents for removal of arsenic from water (Mohan & Pittman 2007; Shakoor *et al.* 2016, 2019). However, iron-coated rice husk biochar (30.7), thiol functionalized sugarcan bagasse (28.57), citric acid modified water melon rind (3.89), modified cassia fistula biochar (0.78), thioglycolated sugarcane carbon (0.08) are used as modified natural adsorbents for removal of arsenic from water (Mohan & Pittman 2007; Shakoor *et al.* 2016, 2019).

In the present work *Phyllanthus emblica*, an excellent fruit popularly known as Indian gooseberry (Annapurn 2012; Zhao *et al.* 2015; Mao *et al.* 2016; Chaphalkar *et al.* 2017) has been utilized first time as a novel adsorbent for removal of As(III) from water in pristine and modified form. *P. emblica* seed coat is derivatized in the form of N-substituted 2-sulfanylacetamide derivative using thioglycolic acid and 1-ethyl-3-(3-dimethylaminopropyl) carbodiimidehydrochloride (EDC). Activated ester leaving group of thioglycolic acid with EDC is displaced by nucleophilic attack of primary amino acids on seed coat. Pristine *P. emblica* (PPE) and derivatized *P. emblica* (DPE) products are characterized using FTIR, SEM-EDX, and XRD techniques. Surface area of the adsorbents can be calculated using BET method. PPE and DPE are applied as adsorbents for removal of trivalent arsenic from water by batch study. The effect of pH of solution, concentration of arsenic ions, adsorbent dose and time of contact are observed for the adsorption efficiency of the adsorbents. This study will be significant for implementation of technology for arsenic remediation in real scenario conditions.

2. MATERIALS AND METHODS

All chemicals and reagents used in the present work were of analytical grade purity and purchased from Central Drug House (CDH) (P) Ltd New Delhi India. Sodium arsenite ($NaAsO_2$) was used for preparing trivalent arsenic ions stock solution. H_2SO_4, EDC, thioglycolic acid ($HSCH_2CO_2H$) were used without further purification for modification of the pristine adsorbent.

2.1. Characterization tools

Mini Flex II XRD manufactured by Regaku (Japan) was employed to measure the X-ray diffraction patterns for the pristine and derivatized *P. emblica* seed coat samples utilized in this research. IR Affinity-1S Shimadzu (Mozambique) instrument was used to measure the spectra of both materials in the middle IR range 4,000–667 cm^{-1} using KBr method. The BET instrument, Micromeritics ASAP 2020 (Germany), porosity and surface analyser, was employed to know the surface area and size of both the sample used in this research through N_2 adsorption. The SEM imaging of samples was carried out using JSM 6510Lv SEM instrument manufactured by Jeol (Japan), operating at an accelerating voltage of 15 kV. 1 cm to 5 μ area may be imaged with magnification 20x-30,000x and spatial resolution of 50–100 nm by using conventional SEM. EDX of adsorbents was carried out by the Oxford INAX-ACT model instrument manufactured by Oxford (London), to know the chemical composition of PPE and DPE. Microwave Plasma-Atomic Emission Spectrophotometer (MP-AES 4200) manufactured by Agilent Technologies Inc. (USA) was used for determination of concentration of arsenic in the solution.

2.2. Preparation of adsorbents

Fresh *P. emblica* was taken from market and its seeds were dried at room temperature for at 48 hours and then crushed to get only the seed coat. Seed coat obtained was further ground into fine powder and then sieved (8″ sieve Mesh no 4). The fine powder of *P. emblica* obtained was then modified in the laboratory with the help of

chemicals to increase the number of cavities for adsorption of arsenic using mentioned process. 1.0 gm of PPE seed coat powder was taken into a round bottom flask. 25 mL methanol, 25 mL of double distilled water, 100 mg EDC, 1 mL double distilled water, 1 mL sulfuric acid and 2 mL thioglycolic acid was added to it. A reflux condenser was attached over the round bottom flask and stirred it for 4 hours on a magnetic stirrer at a temperature of 70–75 °C. After six hours the round bottom flask was removed from magnetic stirrer, cooled and centrifugation was carried out. The residue obtained after filtration was washed 4–5 times with double distilled water and then dried completely. The obtained residue was DPE seed coat powder (Figure 1 (Scheme I)).

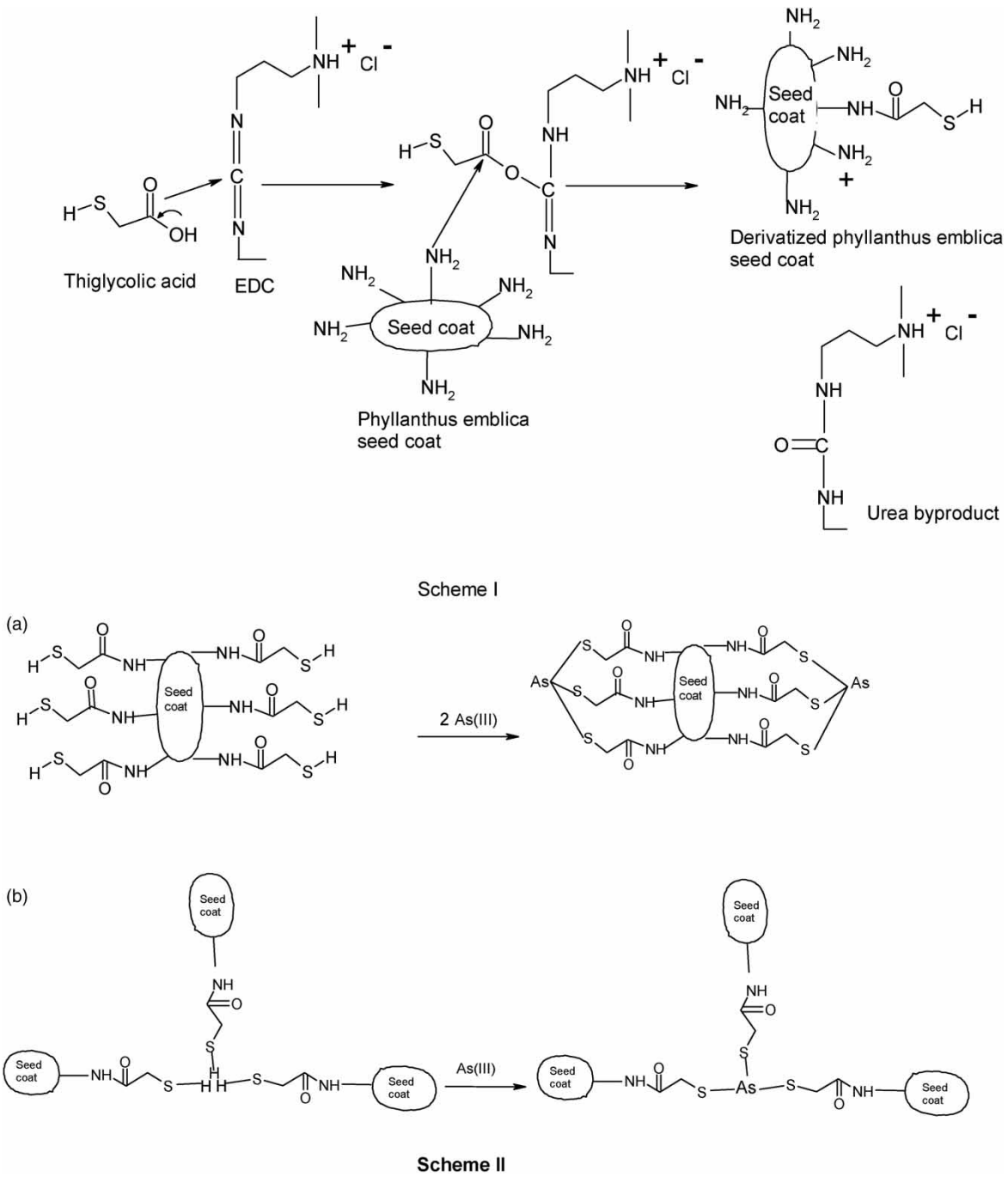

Figure 1 | Schematic diagram (Scheme I) modification of PPE by thioglycolic acid, (Scheme II) trivalent arsenic ions by ion exchange mechanism with DPE.

2.3. Batch studies

A stock solution of 100 ppm trivalent arsenic ions was prepared by utilizing sodium arsenite. The solutions of different concentration required to conduct batch study was obtained from stock solution after dilution. Samples are subjected to atomic emission spectroscopy (AES) to determine the amount of arsenic in the filtrate.

3. RESULTS AND DISCUSSION

3.1. Fourier transform infrared (FTIR) spectral studies

Infrared analysis is used as a characterization technique for identification of the functional groups present in the material and confirmation of modification of adsorbents used in the current study. Pristine (PPE) and derivatized (DPE) compounds show characteristic peaks in the IR spectra (Figure 2). The pristine compound exhibits a broad peak at 3,323 cm^{-1} due to the –OH stretching group present in the compound. The peak at 2,870 cm^{-1} is due to a symmetric stretching peak of the $-CH_2$ group. The peak at 1,359 cm^{-1} is due to a –CH (stretching vibration) group present in the compound whereas peak at 1,703 cm^{-1} is due to C = O (stretching vibration) group present in the compound. The peak at 1,028 cm^{-1} is due to the stretching vibration of C–O (Chen *et al.* 2019). Primary amine shows two weak bands (N–H stretch (asymmetrical), N–H stretch (symmetrical)) in between 3,300 and 3,000 cm^{-1}. These bands are overlapped by O–H stretching appearing in the same region. Thus, equivocal differentiation in structure is sometime impossible. However, secondary amide (RCONHR) shows only a single weak band at 3,275 cm^{-1} because of one N–H bond (Ghosh 2006; Ouellette & Rawn 2014).

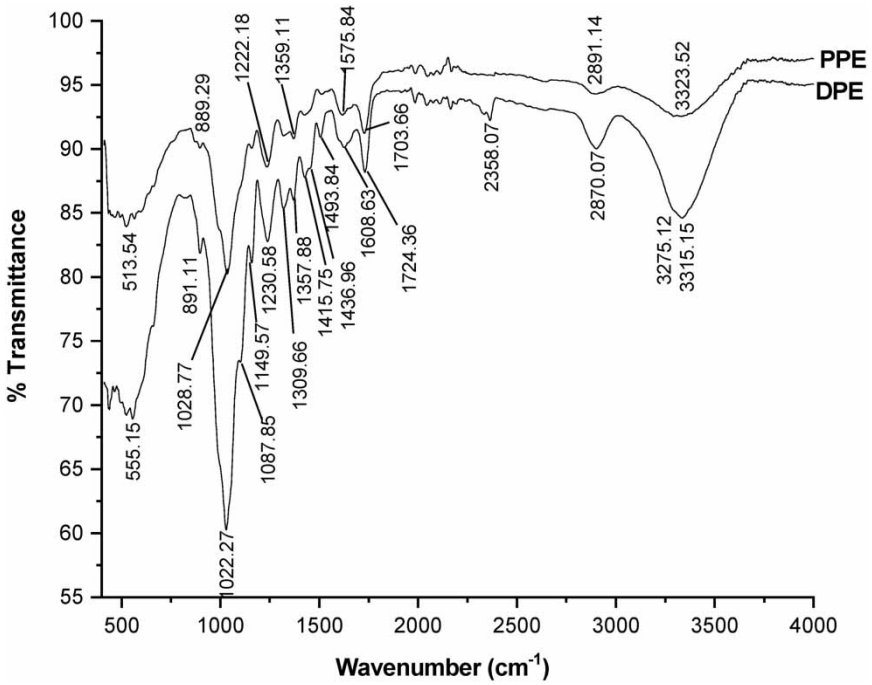

Figure 2 | IR images of (a) PPE and (b) DPE.

The presence of primary amine was confirmed by a weak peak at 1,575 cm^{-1}, which is due to the N–H (bending vibration) group of primary amines. It is deformed in the derivatized (DPE) product at 1,608 cm^{-1} due to modification of the primary amine into amide with the interaction of thioglycolic acid (Zhang *et al.* 2015). More intense peak at 1,222 cm^{-1} represents C–N stretch of aliphatic amines. Also, a weak broad band at 889 cm^{-1} is due to N–H wagging of primary amines. However, it becomes strong broad band for secondary amide at 891 cm^{-1}. The peak at 1,703 cm^{-1} becomes more intense at 1,724 cm^{-1} due to formation of amide stretching vibration of C = O group present in the compound. The weak peak at 2,358 cm^{-1}, is due to the presence of –SH group (Shen *et al.* 2018). A new peak at 1,087 cm^{-1} indicates C–S axial stretching of thioglycolic acid (Papaleo *et al.* 1996).

3.2. X-ray diffraction (XRD) spectral studies

XRD of the pristine (PPE) and derivatized (DPE) products was carried out to determine the crystal structure as well as the chemical composition of sample. The XRD analysis of sample was carried out at 2θ. XRD spectra of pristine as well as modified sample before and after adsorption/removal of arsenic trivalent ions are shown in Figure 3. The sample shows an amorphous hump at about $2\theta = 16.29°$ and a crystalline peak at about $2\theta = 20.99°$. An amorphous hump in the spectrum is due to highly disordered arrangement of the molecules. From the figure, it can be seen that the crystallinity of the sample increases in derivatized (DPE) product. The crystalline peak is more intense in the modified sample (Figure 3(a)). However, the crystallinity of the modified as well as sample is decreased after adsorption of arsenic from water sample (Figure 3(b) and 3(c)).

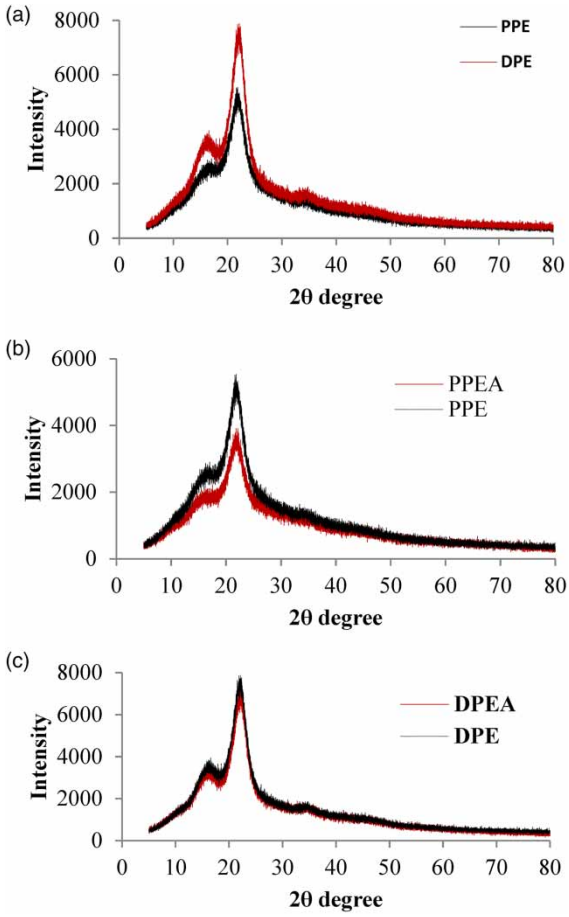

Figure 3 | XRD images of (a) PPE and DPE, (b) PPE and PPEA, (c) DPE and DPEA.

3.3. Scanning electron microscope (SEM) studies

In scanning electron microscopy, a focused beam of electrons interacts with the sample and produces images of the surface of the adsorbent, which gives us information about the topography and composition of the sample. Figure 4(a) and 4(c) show scanning electron microscope images of pristine and derivatized products, whereas Figure 4(b) and 4(d) show SEM images of PPE with arsenic trivalent ions and DPE with arsenic trivalent ions respectively at 2000X magnification. From the figures it can be easily seen that many unoccupied sites in the form of pits or channels are available at the surface of both materials. However, these pits and channels are occupied by the trivalent arsenic ions by the interaction with adsorbent.

3.4. Energy dispersive X-ray spectroscopy (EDX)

EDX provides information about the elemental and chemical composition of PPE and DPE samples. When a high energetic electron beam (HEEB) interacts with samples under investigation, X-rays are emitted from the sample that help to identify the elemental and chemical composition of sample. Emitted X-ray are detected by

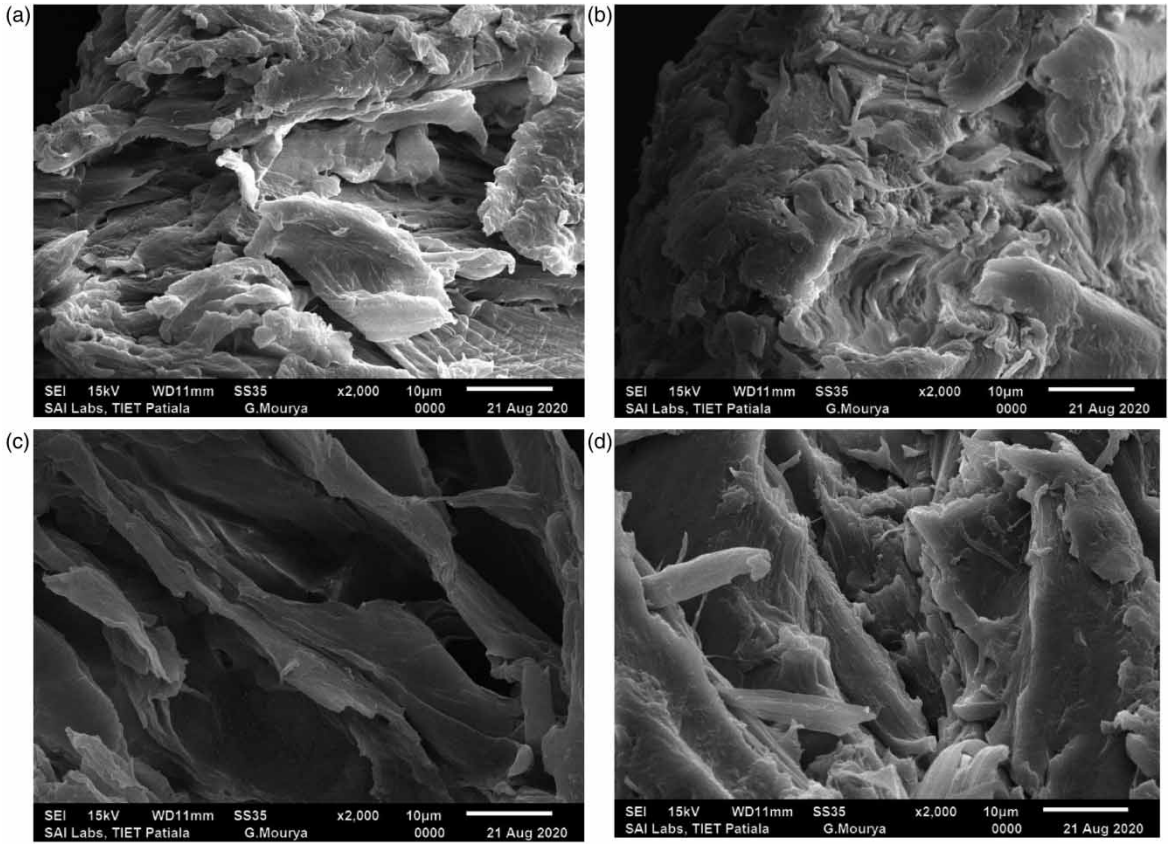

Figure 4 | SEM images of (a) PPE, (b) As(III)-PPE, (c) DPE, (d) As(III)-DPE.

a detector and each X-ray is characteristics for each element present in the sample. It shows the relative abundance of emitted X-rays versus their energy. The EDX spectra of PPE and DPE before and after adsorption are shown in Figure 5. The EDX spectrum of PPE did not display a sulfur peak. However, DPE displayed an additional sulfur peak, which confirmed the presence of sulfhydryl groups. Also, PPE and DPE did not display any elemental arsenic peak. However, after adsorption of arsenic ions both PPE and DPE displayed an additional elemental arsenic peak at 1.22 KeV in the spectrum, which confirmed the presence of arsenic on the surface due to the adsorption process (Figure 5).

3.5. Brunauer, Emmett, and Teller (BET) analysis

The BET t-plot method, an extension of the Langmuir isotherm, was used to find out the specific surface area of PPE and DPE. The properties of PPE and DPE were characterized by utilizing nitrogen gas at an ambient temperature of 22 °C with Micromeritics ASAP 2020, USA. The results showed that the BET surface area (0.3152 ± 0.0081 m^2/g) and Langmuir surface area (0.3571 ± 0.0054 m^2/g) of PPE are changed after modification. DPE showed high surface area compared to un-derivatized adsorbent due to the presence of more modified groups on the surface (BET surface area 0.5812 m^2/g, Langmuir surface area 0.6372 m^2/g).

3.6. Adsorption studies

A batch study was conducted with PPE and DPE product to evaluate the adsorption characteristics in different conditions of concentration of arsenic (20 to 100 mg/L), pH (1 to 9), time of contact (20 to 120 minutes), and adsorbent dose (0.03 to 0.50 g/L). Solutions with the desired concentration of arsenite were prepared from the stock solution of trivalent arsenic using double distilled water. Conical flasks with solutions of different concentrations and specific adsorbent dose were kept over the rotatory shaker for shaking followed by filtration. Filtrate is subjected to AES to determine the amount of arsenic in the filtrate.

To determine the effect of concentration of arsenic on adsorption, different concentrations of arsenic (20 to 100 mg/L) were used at fixed conditions of adsorbent dose, pH dose, contact time, and temperature. Adsorption

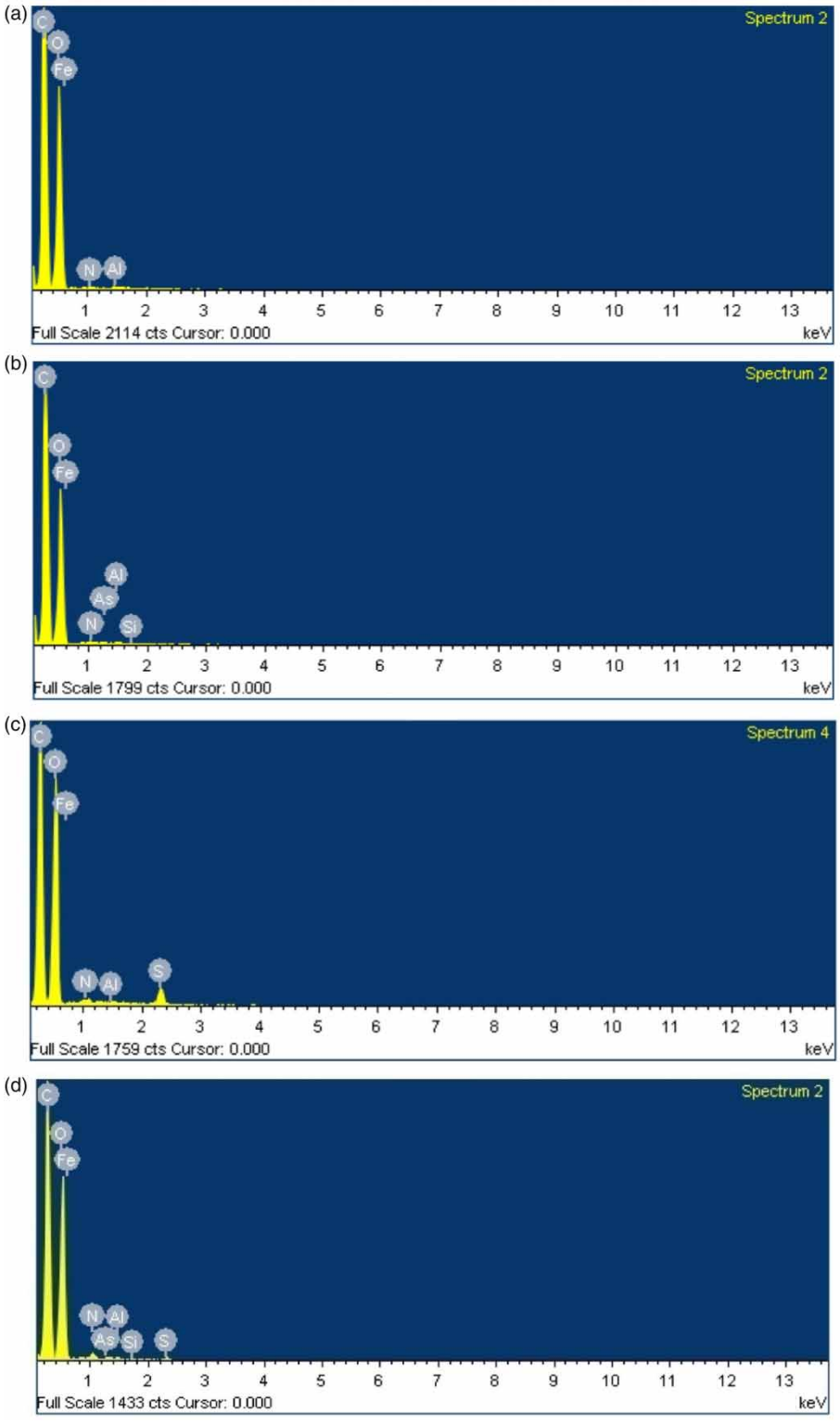

Figure 5 | EDX images of (a) PPE, (b) As(III)-PPE, (c) DPE, (d) As(III)-DPE.

of arsenic ions on the surface of adsorbent was quite significant at lower concentration due to more availability of binding sites on the adsorbent (Figure S1(a)) (Bessaies *et al.* 2020).

To determine the effect of PPE and DPE adsorbent dose on the adsorption, different doses of the adsorbents were used with other factors held constant. 0.03–0.50 g/L of adsorbent was taken into different conical flasks and to each flask 60 mg/L solution of arsenite at other constant conditions was added. Conical flasks with solutions

were kept over the rotatory shaker for shaking then the flasks were removed from the rotatory shaker and filtered. The filtrate is subjected to AES to determine the amount of arsenic in the filtrate. The results showed that with increasing the amount of PPE and DPE adsorbents up to 0.1 g/L, removal of arsenic increases and after that no appreciable increase was observed. The initial rise in adsorption of arsenic is due to more adsorptive sites and a high amount of adsorbent available for adsorption of the ions (Figure S1(b)) (Bessaies *et al.* 2020).

Batch study was conducted at different pH conditions, i.e. 1 to 9, to determine the adsorption of arsenic by the PPE and DPE adsorbents in different media. The pH of solution was maintained by using H_2SO_4 and NaOH. The study was carried out by using 60 mg/L solution of arsenite and 0.06 g/L of adsorbent dose at pH of 1 to 9. Results indicate that adsorption of trivalent arsenic ions was dependent on pH (Figure S1(c)). Removal of trivalent arsenic was found to be increased by a decrease in the acidity of mixture. Maximum removal was achieved in neutral solution (pH 7). Further increase in the basicity of solution arsenic ions caused precipitation in the solution (Yin *et al.* 2022).

To determine the effect of time on adsorption of ions from the prepared solution, different time intervals were taken at other constant factors. Adsorption of arsenic ions increased with increase in the time up to 120 minutes and after that no significant increase was observed for PPE and DPE materials as more sites were available in the beginning of adsorption, which results more adsorption (Figure S1(d)) (Duarte *et al.* 2021). After 120 minutes sites are occupied by the arsenic ions and adsorption becomes almost constant. In case of derivatized material availability of more adsorption groups were leads to increase in the adsorption capacity of the material. So, it can be concluded that pH 7 and contact time of 120 min are favorable conditions for maximum removal from contaminated water with different concentrations of arsenic ions keeping the adsorbent dose from 0.06–0.3 g/L.

3.6.1. Adsorption isotherm

Experiments conducted in batch studies helped to optimize the conditions for adsorption isotherm studies. As the maximum removal was observed in a neutral aqueous sample after 120 minutes. These conditions were selected for further studies taking 0.06 g/L of adsorbent after studying the effect of pH, contact time, and adsorbent dose on removal of arsenic ions from the aqueous sample. Isotherm parameters were obtained by using the well-known Langmuir, Freundlich, and Temkin models. With the help of adsorption isotherms, it can be identified that whether the process of adsorption occurred on a homogenous surface with uni-layered binding or on a heterogeneous surface with multi-layered binding (Kumar & Chawla 2013; Kumar *et al.* 2015; Saini *et al.* 2018, 2019). These isotherms were applied to get the adsorption capacity of *P. emblica* for trivalent arsenic ions.

3.6.2. Langmuir isotherm

Experimental runs were conducted under optimized conditions (pH 7, contact time 120 minutes and adsorbent dose 0.06 g/l). Langmuir isotherm assumes that the adsorption takes place on the homogenous surface with uni-layered binding without any linkage with the sorbed material and it is given as:

$$q_e = \frac{q_{max} \mathrm{K_L} C_e}{1 + \mathrm{K_L} C_e} \tag{1}$$

where C_e is the amount of trivalent arsenic ions at equilibrium, $\mathrm{K_L}$ constant is Langmuir constant and q_{max} shows the maximum adsorption capacity of *P. emblica* in mg/g, q_e is amount of adsorbed trivalent arsenic ions (mg/g) at equilibrium. The Langmuir isotherm is used to define a separation factor $\mathrm{R_L}$. The value of $\mathrm{R_L}$ indicates that whether the adsorption is taken place under favourable or unfavourable conditions.

$$\mathrm{R_L} = \frac{1}{1 + \mathrm{K_L} C_o} \tag{2}$$

Zero value of $\mathrm{R_L}$ indicates irreversible isotherm; whereas unity indicates the linear isotherm, However, if $\mathrm{R_L}$ has less than one but greater than zero isotherm will be favorable and if $\mathrm{R_L}$ has greater than one isotherm will be unfavorable and for both of the adsorbents $\mathrm{R_L}$ values were found to $0 < \mathrm{R_L} < 1$ for all experiments, indicating favorability of the isotherm (Table 1). q_{max} in mg/g and another constant calculated by using slope and intercept of the linear plot of C_e versus C_e/q_e (Table 1 and Figure 6(a)). The Langmuir q_{max} for PPE and DPE were observed to be 76.92 and 90.90 mg/g respectively.

Table 1 | Three isotherms for q_{max} and other constants of arsenic ions on PPE and DPE

	Isotherm model							
	Langmuir			Freundlich			Temkin	
Adsorbent	q_{max} (mg/g)	R_L (l/g)	R^2	n	kf	R^2	B	R^2
PPE	76.92	0.0143	0.998	1.40	1.92	0.995	14.26	0.986
DPE	90.90	0.0148	0.999	1.36	2.22	0.996	16.73	0.982

3.6.3. Freundlich isotherm

The data were also fitted with the Freundlich isotherm model to check the heterogeneity of the adsorbent surface. Freundlich isotherm is applicable when the adsorption occurs on a heterogeneous surface with multilayer binding. Freundlich equation is expressed as:

$$q_e = \mathrm{k_f} C_e^{1/n} \tag{3}$$

where $\mathrm{k_f}$ is Freundlich constant; $1/n$ is the heterogeneity of the adsorbent surface and distribution of energy. lnkf and 1/n can be obtained using the intercept and slope of the linear plot of $\ln C_e$ and $\ln q_e$ respectively. $1/n < 1$

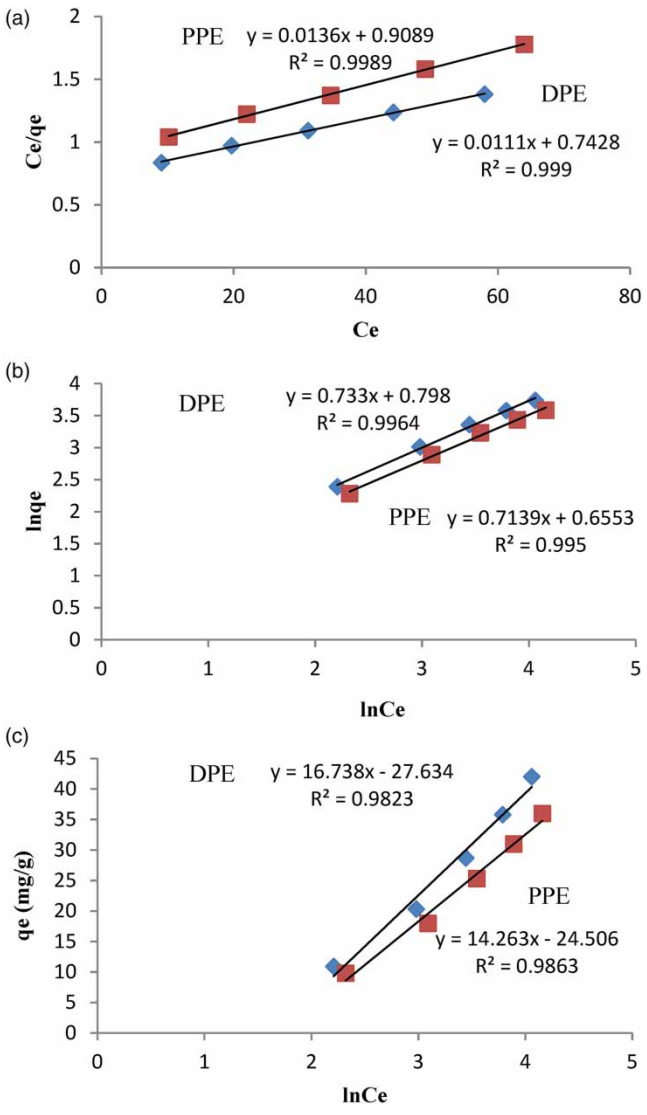

Figure 6 | Isotherm models, (a) Langmuir, (b) Freundlich, (c) Temkin for removal of trivalent arsenic ions by using PPE and DPE.

represents normal adsorption; $1/n > 1$ represents favorable adsorption and called as cooperative adsorption. All the calculated values from graph are summarized in Table 1. $1/n < 1$ indicates normal adsorption. The smaller value of $1/n < 1$ also indicates highly heterogeneou adsorbent surface (Figure 6(b)).

3.6.4. Temkin isotherm

The adsorption potential of adsorbent/adsorbate interactions can also be evaluated by the Temkin isotherm, which explicitly takes into account the interactions of adsorbate ions of the solution and the surface of the adsorbent. It can be described as follows:

$$q_e = \mathrm{b} \ln \mathrm{AC_e} \tag{4}$$

where b and A (L/min) are constant and equilibrium binding constant respectively. The value of b can be evaluated by $\mathrm{b} = \mathrm{RT/B}$, B is the Temkin constant (heat of sorption (J/mol)), R (ideal gas constant) and T (temperature).

The value of b and A (L/min) can be calculated using intercept and slope of the linear plot of $\mathrm{q_e}$ versus $\ln \mathrm{C_e}$ (Figure 6(c)). The results are summarized in Table 1. The value of B was found to be 14.26 J/mol for pristine material and 16.73 J/mol for derivatized material indicating physical adsorption on the surface of adsorbents. However, the low values of b represent a feeble interaction between trivalent arsenic and both adsorbents, which sometimes favors ion exchange mechanism.

3.6.5. Kinetics of adsorption

The rate of adsorption of arsenic on *P. emblica* adsorbents were studied by using time-dependent data. Time-dependent data were obtained from 20 to 120 minutes' time duration at optimum dose of adsorbent and optimum concentration of arsenic ions at normal temperature. In the initial stage of time (15 to 20 minutes) fast removal of arsenic ions was achieved due to availability of active sites. The progress of removal after 20 minutes was quite slow due to occupation of the active sites by the arsenic ions. Time dependent data were also analyzed by using pseudo-first- and second-order kinetics models to known the mechanism of reaction, i.e. physiosorption or chemisorptions.

3.6.5.1. Pseudo-first-order and pseudo-second-order kinetic model. To determine rate of adsorption of arsenic pseudo-first-order kinetic model is expressed as:

$$dq_t/dt = \mathrm{k_1}(q_e - q_t) \tag{5}$$

Pseudo-second-order equation is represented as:

$$dq_t/dt = \mathrm{k_2}(q_e - q_t)^2 \tag{6}$$

where $\mathrm{k_1}$ and $\mathrm{k_2}$ (L/mg/min) are first- and second-order rate constants, q_e and q_t are equilibrium amount adsorbed at time t (mg/g) and at time $t = \infty$ respectively. The value of both can be obtained from batch study conducted during the experimentation. Adsorption capacity at equilibrium and rate constant were evaluated from the linear plot of $\ln(q_e - q_t)$ versus t. The value of $\mathrm{k_1}$ (rate constant) can be evaluated by the slope of the linear plot of $\ln(q_e - q_t)$ versus t and the q_e and $\mathrm{k_2}$ (rate constant) can be evaluated from the slope and intercept of plot of t/qt versus t (Figure 7(a) and 7(b)).

The value of q_e, $\mathrm{k_1}$, q_e, and $\mathrm{k_2}$ are tabulated in Table 2. The value of regression correlation coefficient ($\mathrm{R^2}$) confirmed that pseudo-second-order reaction kinetics model was the best fitted model and the value of calculated adsorption capacity at equilibrium was 27.77 and 31.25 mg/g for pristine and derivatized material respectively. This value was very close to experimental value for both of the adsorbents.

3.7. Proposed mechanism

Fruit pulp, seed coat and seed are the main parts of the *P. emblica* fruit. Fat, proteins, primary aliphatic or aromatic amino acids, carbohydrates, pectic substances, gallic acid and tannic acids (phenolic acids), and crude fibers are the main components of seed coat of *P. emblica*. Octadeca-9,12,15-trienoic acid, long chain fatty acid tetradecanoic acid and octadecadienoate (linoleates) were the major components in seed coat oil (Khan

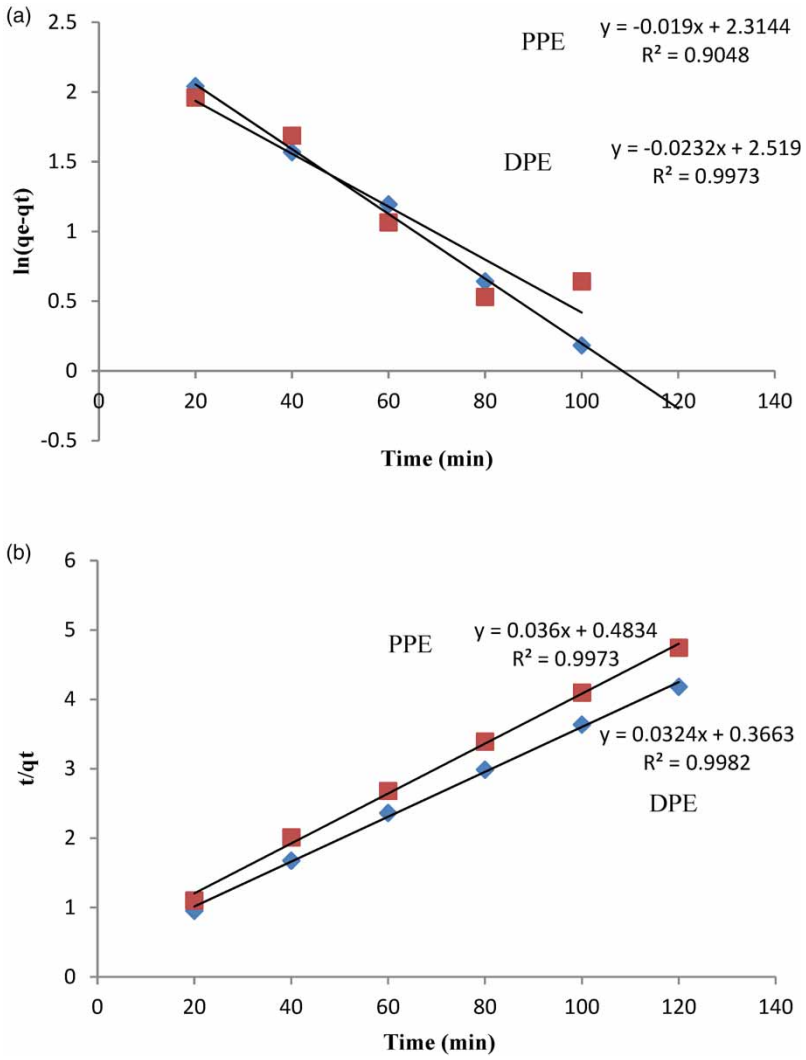

Figure 7 | Kinetic models (a) pseudo-first order, (b) pseudo-second order, models for trivalent arsenic ions on PPE and DPE.

Table 2 | Adsorption kinetics of arsenic (III) ions on PPE and DPE

	Pseudo kinetics						
	First-order			Second-order			
Adsorbent	q_e	k_1	R^2	q_e	k_2	R^2	q_e, exp. (mg/g)
PPE	10.11	0.019	0.904	27.77	0.0027	0.997	25.3
DPE	12.41	0.023	0.997	31.25	0.0028	0.998	28.7

2009; Rai *et al.* 2012; Hasan *et al.* 2016; Variya *et al.* 2016; Kulkarni & Ghurghure 2018). Carboxylic group of thioglycolic acid reacts with EDC to form an activated ester leaving group, which is displaced by nucleophilic attack of primary aliphatic or aromatic amino acids on *P. emblica* seed at pH 4.0–6.0. EDC is released as soluble urea by product derivative (Figure 1 (Scheme I)). Trivalent arsenic has high affinity for sulfhydryl groups. One arsenic trivalent ion binds with three sulfhydryl groups (Figure 1 Scheme II). There may be two possibilities of binding the arsenic trivalent ions with sulfhydryl groups, one is that it may bind with sulfhydryl groups of the same unit and in another case the three sulfhydryl groups are from three different units (Figure 1 Scheme II (A&B)). Removal of the arsenic from water depends on the availability of binding sites of the adsorbent. Removal of arsenic by the derivatized material was also facilitated by binding with the sulfhydryl groups (Mohan & Pittman 2007; Shen *et al.* 2013; Ko *et al.* 2017). Thus, derivatized material showed more adsorption capacity than the

pristine material because of more favourable binding positions on the surface of the adsorbent (Duarte *et al.* 2021).

3.8. Regeneration of the adsorbents

Recycling of applied adsorbents and recovery of the arsenic ions from the desorbing agents is one of the most important parts of adsorption study to keep the environment and human beings safe and healthy. It is also very important to reduce the cost of the method. Both adsorbents were regenerated by designing column study using 30% H_2O_2 in 0.1 M HNO_3 followed by 0.1M NaOH solution (Natale *et al.* 2013; Lata *et al.* 2014). After regeneration both materials were washed with double distilled water and dried at 120 °C overnight, and stored for further use. The Langmuir q_{max} after regeneration of the PPE was observed 62.11 and for DPE 77.51 mg/g respectively. Thus, 80.74% for PPE and 85.27% for DPE efficiency was achieved in the first cycle for desorbing process (Figure S3).

3.9. Column study using PPE and DPE

Column study was performed using PPE and DPE adsorbent as a fixed bed packing in the column of 25 mL capacity, having the length 79.75 cm, outer diameter 1.4 cm, inner diameter 0.8 cm at a constant flow rate of 5 mL/minute for 20 mL synthetic arsenic solution. 2 mg/L aqueous arsenic solution at pH 7 was passed through the column packed with PPE and DPE adsorbents to check the applicability of the used materials. Column was prepared by taking glass column packed with PPE/DPE up to 5 cm. Glass wool was placed at the end of the column and at the top of the column to prevent the loss of the adsorbent (Figure S2). The column was preconditioned with double-distilled water. More than 98% efficiency was observed for PPE and 100% efficiency for DPE in the consecutive steps. No arsenic was found after passing through column with both of the adsorbents. Optimization plays a key role for treatments of ground as well as wastewater. Various combinations of parameters can be set by using the optimization results for maximum removal of arsenic from various water samples. These materials can be applied as a packing material in the column for real water samples with knowing the other characteristics conditions of the water samples.

3.10. Performance analysis of *P. emblica* adsorbent with other adsorbents

It is significant to evaluate the active performance of novel adsorbents used in the study with other reported materials keeping in view of accessibility, usability, and adsorption capacity. Numerous synthetic, natural, and modified materials have been applied as adsorbents for removal of heavy metals and arsenic trivalent ions. However, utilization of some materials is still less due to low adsorption capacities and lack of regeneration studies or reuse capacity of the materials.

A review was carried out to check the potency of current adsorbents (pristine and modified) for the removal/adsorption of trivalent arsenic in solution. Adsorption/removal of trivalent arsenic ions has been studied using broad range of natural adsorbents in their pristine and modified form. On investigating the reported papers, maximal adsorption capacities (q_{max}) for uptake of trivalent arsenic ions from aqueous media by pristine as well as by modified materials at given sets of performing conditions followed the below given order (Figure 8(a)): For unmodified (pristine) adsorbents: *P. emblica* seed coat (PPE) 76.92 > *Acacia nilotica* (AN) 50.8 > *A. auriculiformis* leaf (AAL) 41.41 > rice husk biochar (RHB) 19.3 > egg shell (ES) 11.69 > *Hydrilla verticilata* (HV) 11.65 > water chestnut shell (WCS) 9.61 > tea waste (TW) 7.36 > pomegranate peel (PP) 5.57 > java plum seed (JPS) 4.63 > corn cob (CC) 4.33 > water melon rind (WMR) 3.4 > bagasse (Bag) 1.35 > mango bark (MB) 1.25 > sugarcane bagasse (SCB) 1.20 > orange peel (OP) 1.08 > guava leaf biomass (GLB) 1.05 > psidium guajava (PG) 1.06 > biochar of rice straw (BCRS) 0.44 > momordicacharantia (MC) 0.88 > banana peel (BP) 0.84 > rice polish (RP) 0.04 (Mohan & Pittman 2007; Shakoor *et al.* 2016, 2019).

Similarly, uptake capacity of modified adsorbents is specified below(Figure 8(b)): For modified adsorbents: DPE seed coat 90.90 mg/g > Fe-coated EFBB (FC-EFBB) 31.4 > Fe coated rice husk biochar (FC-RHB) 30.7 > thiol functionalized sugarcan bagasse (TFSCB) 28.57 > xanthated water melon rind (X-WMR) 3.96 > citric acid modified water melon rind (CA-WMR) 3.89 > Japanese oak wood-derived biochar (OW-BC) 3.21 > acid treated longifolia leaf powder (ATLP) 1.51 > modified *Cassia fistula* biochar (MCFB) 0.78 > nanoporous activated garlic stem carbon (AGSC) 0.19 > thioglycolated sugarcane carbon (TSCC) 0.08 (Mohan & Pittman 2007; Shakoor *et al.* 2016, 2019).

The study reveals that *P. emblica* seed coat and its modified form are very good adsorbents with very high adsorption capacity compared to many natural and modified materials shown in Figure 8. The reason of high

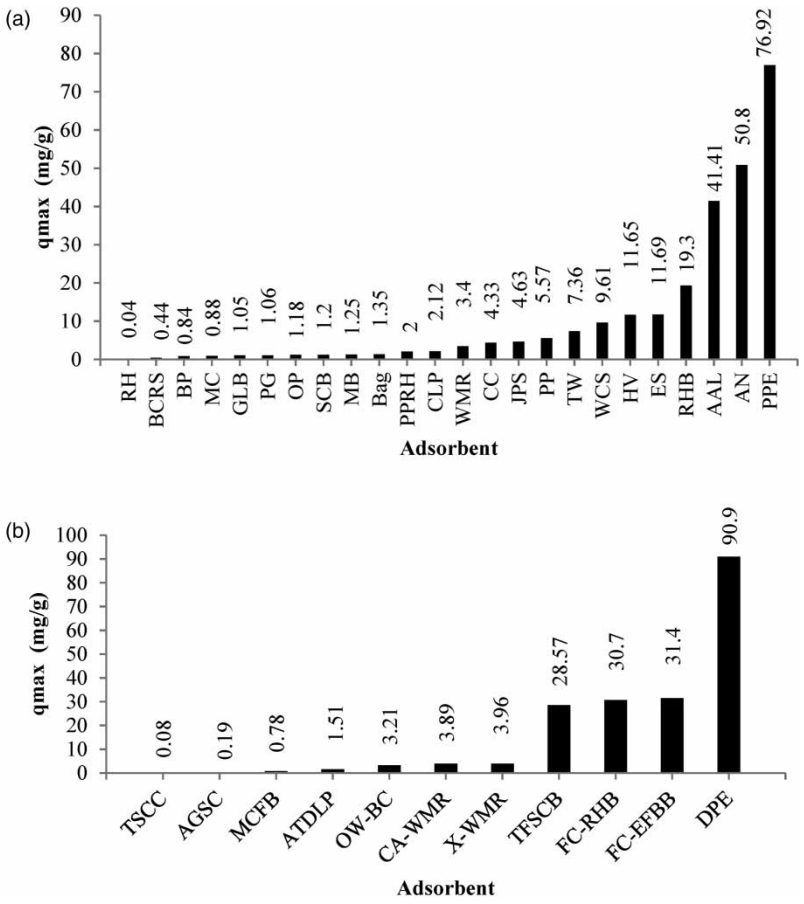

Figure 8 | Assessment diagram (a) *P. emblica* seed coat adsorbent with other adsorbents (b) DPE seed coat adsorbent with other adsorbents.

adsorption capacity of these adsorbents are presence of more and more binding sites on the surface and high affinity of arsenic trivalent ions for sulfhydryl groups in modified form.

4. CONCLUSION

In this paper PPE seed coat were modified in the form of N-substituted derivative of 2-sulfanylacetamide by using thioglycolic acid and EDC. IR, SEM, EDX, and XRD techniques were applied for characterization of PPE and DPE products. A weak peak at 1,575 cm^{-1} (N–H bending) in infra red is deformed at 1,608 cm^{-1} in the modified product due to modification of the primary amine into amide with the interaction of thioglycolic acid. Both novel materials were used for adsorption or removal of trivalent arsenic from water medium. Significant change was observed in derivatized product DPE because of presence of high affinity groups towards trivalent arsenic ions. The Langmuir q_{max} for PPE and DPE were observed to be 76.92 and 90.90 mg/g respectively. These materials can be applied as a packing material in the column for real water sample as well as for wastewater treatment under a given set of conditions to remove arsenic along with other ions.

ACKNOWLEDGEMENTS

This work was supported by management of Manav Rachna International Institute of Research and Studies Faridabad, Haryana, India.

DATA AVAILABILITY STATEMENT

All relevant data are included in the paper or its Supplementary Information.

CONFLICT OF INTEREST

The authors declare there is no conflict.

REFERENCES

Alka, S., Shahir, S., Ibrahim, N., Ndejiko, M. J., Vo, D.-V. N. & Manan, F. A. 2021 Arsenic removal technologies and future trends: a mini review. *Journal of Cleaner Production* **278**, 123805.

Annapurn, A. 2012 Health benefits of amla or Indian gooseberry fruit (Phyllanthus emblica). *Asian Journal of Pharmaceutical Research and Health Care (AJPRHC)* **4**(4), 93.

Bagchi, S. 2007 Arsenic threat reaching global dimensions. *Canadian Medical Association Journal* **177**(11), 1344–1345.

Balsamo, M., Natale, F. D., Erto, A., Lancia, A., Montagnaro, F. & Santoro, L. 2010 Arsenate removal from synthetic wastewater by adsorption onto fly ash. *Desalination* **263**(1–3), 58–63.

Bessaies, H., Iftekhar, S., Doshi, B., Kheriji, J., Ncibi, M. C., Srivastava, V., Sillanp, M. & Hamrouni, B. 2020 Synthesis of novel adsorbent by intercalation of biopolymer in LDH for the removal of arsenic from synthetic and natural water. *Journal of Environmental Sciences* **91**, 246–261.

Chaphalkar, R., Apte, K. G., Talekar, Y., Ojha, S. K. & Nandave, M. 2017 Antioxidants of phyllanthus emblica L. bark extract provide hepatoprotection against ethanol-Induced hepatic damage: a comparison with silymarin. *Oxidative Medicine and Cellular Longevity* **2017**, 3876040.

Chen, K., Zhang, Z., Xia, K., Zhou, X., Guo, Y. & Huang, T. 2019 Facile synthesis of thiol-functionalized magnetic activated carbon and application for the removal of mercury(II) from aqueous solution. *ACS Omega* **4**(5), 8568–8579.

Duarte, G., Teixeira, M. C., Olusegun, S. J. & Ciminelli, V. S. T. 2021 Mechanisms of arsenic removal from simulated surface water based on As(III) retention on thiol chelating resins. *Environmental Nanotechnology, Monitoring & Management* **16**, 100532.

Ghosh, S. K. 2006 *Advanced General Organic Chemistry – A Modernapproach. UV–Visible and IR Spectroscopy*, 2nd edn. NewCentral Book Agency, Kolkata, p. 371.

Gramling, C. 2020 Available from: https://www.sciencenews.org/article/arsenic-contamination-drinking-water-global-map-risk (May 21, 2020)

Hasan, M. R., Islam, M. N. & Islam, M. R. 2016 Phytochemistry, pharmacological activities and traditional uses of Emblica officinalis: a review. *International Current Pharmaceutical Journal* **5**(2), 14–21.

Hu, J. L., Yang, X. S., Liu, T., Shao, L. N. & Zhang, W. 2017 Dynamic desorption of arsenic from polymer-supported hydrated iron(III) oxide in a wastewater treatment plant. *Water Science and Technology* **76**(9), 2380–2388.

India Today Web Desk 2018 https://www.indiatoday.in/education-today/gk-current-affairs/story/1-47-crore-indians-at-high-risk-of-cancer-due-to-arsenic-contaminated-water-1368198-2018-10-15 (October 15, 2018).

Jadhav, R. 2017 https://timesofindia.indiatimes.com/india/19-of-indians-drink-water-with-lethal-levels-of-arsenic/articleshow/62226542.cms (Dec 24, 2017).

Kanel, S. R., Manning, B., Charlet, L. & Choi, H. 2005 Removal of Arsenic(III) from Groundwater by Nanoscale Zero-Valent Iron, *Environmental Science & Technology* **39** (5), 1291–1298.

Khan, K. H. 2009 Roles of emblica officinalis in medicine – A review. *Botany Research International* **2**(4), 218–228.

Ko, D., Lee, J. S., Patel, H. A., Jakobsen, M. H., Hwang, Y., Yavuz, C. T., Hansen, H. B., Henrik & Andersen, H. R. 2017 Selective removal of heavy metal ions by disulfide linked polymer networks. *Journal of Hazardous Materials* **332**, 140–148.

Kulkarni, K. V. & Ghurghure, S. M. 2018 Indian gooseberry (Emblica officinalis): complete pharmacognosy review. *Journal of Chemistry Studies* **2**(2), 5–11.

Kumar, R. & Chawla, J. 2013 Removal of cadmium ion from water/wastewater by nano-metal oxides: a review. *Water Quality, Exposure and Health* **5**(4), 215–226.

Kumar, R., Chawla, J. & Kaur, I. 2015 Removal of cadmium ion from wastewater by carbon-based nanosorbents: a review. *Journal of Water and Health* **13**(1), 18–33.

Lata, S., Singh, P. K. & Samadder, S. R. 2015 Regeneration of adsorbents and recovery of heavy metals: a review. *International Journal of Environmental Science and Technology*, **12**(4), 1461–1478.

Ladeira, A. C. Q. & Ciminelli, V. S. T. 2004 Adsorption and desorption of arsenic on an oxisol and its constituents. *Water Research* **38**(8), 0–2094.

Lenoble, V., Chabroullet, C., Al-Shukry, R., Serpaud, B., Deluchat, V. & Bollinger, J. C. 2004 Dynamic arsenic removal on a MnO2-loaded resin. *Journal of Colloid and Interface Science* **280**(1), 62–67.

Lin, T. F. & Wu, J. K. 2001 Adsorption of arsenite and arsenate within activated alumina grains: equilibrium and kinetics. *Water Research* **35**(8), 2049–2057.

Mandal, B. & Suzuki, K. T. 2002 Arsenic round the world: a review. *Talanta* **58**(1), 201–235.

Mao, X., Wu, L.-F., Guo, H.-L., Chen, W.-J., Cui, Y.-P., Qi, Q. & Zhang, L.-Z. 2016 The genus phyllanthus: an ethnopharmacological, phytochemical, and pharmacological review. *Evidence-Based Complementary and Alternative Medicine* **2016**, 7584952.

Martinson, C. A. & Reddy, K. J. 2009 Adsorption of arsenic(III) and arsenic(V) by cupric oxide nanoparticles. *Journal of Colloid and Interface Science* **336**, 406–411.

Mohan, D. & Pittman, C. U. 2007 Arsenic removal from water/wastewater using Adsorbents A critical review. *Journal of Hazardous Materials* **142**(1–2), 1–53.

Natale, F. D., Erto, A. & Lancia, A. 2013 Desorption of arsenic from exhaust activated carbons used for water purification. *Journal Hazardous Material* **15**(260), 451–458.

Nicomel, N. R., Leus, K., Folens, K., Van Der Voort, P. & Du Laing, G. 2016 Technologies for arsenic removal from water: current status and future perspectives. *International Journal of Environmental Research and Public Health* **13**(1), 62.

Osuna-Martínez, C. C., Armienta, M. A., Bergés-Tiznado, M. E. & Páez-Osuna, F. 2021 Arsenic in waters, soils, sediments, and biota from Mexico: an environmental review. *Science of The Total Environment* **752**, 142062.

Ouellette, R. J. & Rawn, D. 2014 *Chapter 2 – Part I: Functional Groups and Their Properties Organic Chemistry Structure, Mechanism, and Synthesis*, 1st edn, pp. 41–74.

Palma-Lara, I., Martínez-Castillo, M., Quintana-Pérez, J. C., Arellano-Mendoza, M. G., Tamay-Cach, F., Valenzuela-Limón, O. L., García-Montalvo, E. A. & Hernández-Zavala, A. 2020 Arsenic exposure: a public health problem leading to several cancers. *Regulatory Toxicology and Pharmacology* **110**, 104539.

Papaleo, R. M., Hallen, A., Sundqvist, B. U. R., Farenzena, L., Livi, R. P., deAraujo, M. A. & Johnson, R. E. 1996 Chemical damage in poly(phenylenesulphide) from fast ions: dependence on the primary-ionstopping power. *Physical Review B* **5**, 2303–2313.

Pirilä, M., Martikainen, M., Ainassaari, K., Kuokkanen, T. & Keiski, R. L. 2011 Removal of aqueous As(III) and As(V) by hydrous titanium dioxide, *Journal of Colloid and Interface Science* **353**, (1), 257-262.

Prasad, B., Ghosh, C., Chakraborty, A, Bandyopadhyay, N. & Ray, R.K. 2011 Adsorption of arsenite (As3+) on nano-sized Fe2O3 waste powder from the steel industry, *Desalination* **274**, (1–3), 105-112.

Rai, N., Tiwari, L., Sharma, R. K. & Verma, A. K. 2012 Pharmaco-botanical profile on emblica officinalis Gaertn. *A Pharmacopoeial Herbal Drug. STM Journals* **1**(1), 29–41.

Saini, S., Kumar, R., Chawla, J. & Kaur, I. 2018 Punica granatum (pomegranate) carpellary membrane and its modified form used as adsorbent for removal of cadmium (II) ions from aqueous solution. *Journal of Water Supply: Research and Technology – Aqua* **67**(1), 68–83.

Saini, S., Kumar, R., Chawla, J. & Kaur, I. 2019 Adsorption of bivalent lead ions from an aqueous phase system: equilibrium, thermodynamic, kinetics and optimization studies. *Water Environment Research* **91**(12), 1692–1704.

Shaji, E., Santosh, M., Saratha, K. V., Prakash, P., Deepchand, V. & Divya, B. V. 2020 *Arsenic Contamination of Groundwater: A Global Synopsis with Focus on the Indian Peninsula Geoscience Frontiers*.

Shakoor, M. B., Niazi, N. K., Bibi, I., Murtaza, G., Kunhikrishnan, A., Seshadri, B., Shahid, M., Ali, S., Bolan, N. S., Ok, Y. S., Abid, M. & Ali, F. 2016 Remediation of arsenic-contaminated water using agricultural wastes as biosorbents. *Journal Critical Reviews in Environmental Science and Technology* **46**(5), 467–499.

Shakoor, M. B., Niazi, N. K., Bibi, I., Shahid, M., Saqib, Z. A., Nawaz, M. F., Shaheen, S. M., Wang, H., Daniel, C. W., Bundschuh, T. J., Ok, Y. S. & Rinklebe, J. 2019 Exploring the arsenic removal potential of various biosorbents from water. *Environment International* **123**, 567–579.

Shen, S., Li, X. F., Cullen, W. R., Weinfeld, M. & Le, X. C. 2013 Arsenic binding to proteins. *Chemical Reviews* **113**(10), 7769–7792.

Shen, Y., Jiang, N., Liu, S., Zheng, C., Wang, X., Huang, T., Guo, Y. & Bai, R. 2018 Thiol functionalization of short channel SBA-15 through a safe, mild and facile method and application for the removal of mercury (II). *Journal of Environmental Chemical Engineering* **6**(4), 5420–5433.

Thirunavukkarasu, O. S., Viraraghavan, T., Subramanian, K. S., Chaalal, O. & Islam, M. R. 2005 Arsenic removal in drinking water – impacts and novel removal technologies. *Energy Sources* **27**(1–2), 209–219.

USEPA 2001 National primary drinking water regulations: arsenic and clarifications to compliance and new source contaminants monitoring, in: Final Rule, Code of Federal Regulations, title 40, parts 141–142.

Variya, B. C., Bakrania, A. K. & Patel, S. S. 2016 Emblica officinalis (Amla): a review for its phytochemistry, ethnomedicinal uses and medicinal potentials with respect to molecular mechanisms. *Pharmacological Research* **111**, 180–200.

Vunain, E., Mishra, A. K. & Krause, R. W. 2013 Fabrication, Characterization and Application of Polymer Nanocomposites for Arsenic (III) Removal from Water, *Journal of Inorganic and Organometallic Polymers and Materials* **23**(2), 293–305.

World Health Organization (WHO) 2011 In: *Arsenic in Drinking Water* (World Health Organization ed.). WHO, Geneva, Switzerland.

Yin, C., Li, S., Liu, L., Huang, Q., Zhu, G., Yang, X. & Wang, S. 2022 Structure-tunable trivalent Fe-Al-based bimetallic organic frameworks for arsenic removal from contaminated water. *Journal of Molecular Liquids* **346**, 117101–117112.

Zhang, J., Ding, T., Zhang, Z., Xu, L. & Zhang, C. 2015 Enhanced adsorption of trivalent arsenic from water by functionalized diatom silica shells. *PLOS ONE* **10**(4), 1–18.

Zhao, T., Sun, Q., Marques, M. & Witcher, M. 2015 Anticancer properties of phyllanthus emblica (Indian gooseberry). *Oxidative Medicine and Cellular Longevity* **2015**, 950890.

First received 10 December 2021; accepted in revised form 6 July 2022. Available online 13 July 2022